Effect of End-Anchored Chains on the Adhesion at a Thermoset–Thermoplastic Interface

L. J. Norton,[†] V. Smigolova,[‡] M. U. Pralle,[§] A. Hubenko,[∥] K. H. Dai,[⊥] and E. J. Kramer*

Department of Materials Science and Engineering and Materials Science Center, Cornell University, Ithaca, New York 14853

S. Hahn, C. Berglund, and B. DeKoven

Central Research and Development, Dow Chemical Company, Midland, Michigan 48674

Received August 23, 1994; Revised Manuscript Received December 1, 1994[⊗]

ABSTRACT: The asymmetric double cantilever beam fracture test was used to measure the critical energy release rate, or fracture toughness, G_c, of an epoxy–polystyrene (PS) interface as a function of the grafting density, Σ, and degree of polymerization, N, of carboxylic acid terminated deuterated polystyrene chains (dPS-COOH). The chain ends anchor to the epoxy, and their tails penetrate into the PS homopolymer. Forward recoil spectrometry (FRES) on the fracture surfaces provided a method to determine the total Σ as well as the mechanism of interface failure. For $N = 159$ the grafted chains were too short to entangle and pull out of the PS, leading to no enhancement in G_c over that of a bare interface. When the chain length was increased to $N = 412$ and 535, there was sufficient stress transfer to initiate crazes in the PS that break down by either disentanglement or scission of dPS-COOH chains in the craze fibrils. For long, well-entangled chains of $N = 688$, 838, and 1478 the chains broke near the epoxy–PS interface at low Σ before significant crazing of the PS occurs. A transition from chain scission to crazing occurred at $\Sigma_c = 0.03$ chains/nm^2 for all three chain lengths, agreeing with experiments on diblock copolymer modified thermoplastic–thermoplastic interfaces[1] and with the prediction from the fracture mechanism map[2] that the transition is independent of chain length. We observed a nearly linear decrease in the maximum achievable Σ as N increased that can be explained in part by an entropic barrier that opposes the addition of new chains to the grafted brush. The toughest interfaces occurred with intermediate length grafted chains, $N = 838$, when the chains were well entangled and the grafted brush was dense enough, $\Sigma > \Sigma_c$, to cause energy dissipation through craze formation.

1. Introduction

Interface adhesion has important consequences in many technologically critical areas. For example the interface impacts the toughness of rubber-modified glassy polymers, the success of lamination in polymer composites such as printed circuit boards, and the efficacy of polymer coatings such as paint to plastic parts. Mechanisms to improve adhesion with polymers may rely upon interpenetration of molecules across the interface or the complexation/reactivity between the two layers, often enhanced by the addition of a dopant *adhesion promoter*. Through controlled experiments on an isolated interface, correlations can be made between the microscopic interface structure and the adhesion. An asymmetric double cantilever beam technique has been developed[3] and applied extensively to measure the adhesion of planar interfaces between immiscible polymers[4–6] and at polymer/nonpolymer interfaces[7,8] modified with diblock copolymers as well as with alternative architectures such as random copolymers.[9–11] Substantial advances have been made in these and related studies on understanding the microscopics of the interface failure by combining the fracture test with methods for locating the labeled copolymer after fracture such as forward recoil spectrometry (FRES), Rutherford back-scattering (RBS), secondary ion mass spectrometry (SIMS), and X-ray photoelectron spectrometry (XPS). In this paper we present an experimental study of a thermoset–thermoplastic interface modified with chains end-anchored to the thermoset. As the degree of polymerization N of the grafted chains increases, their tail becomes progressively more entangled with the thermoplastic and different failure mechanisms are observed.

The fracture mechanism map[2] shown in Figure 1 predicts that the interface modified with short grafted chains will fail by pull out of the grafted chains from the thermoplastic when a stress, $\sigma_{pullout}$, is reached. This stress depends linearly on the degree of polymerization N, the areal density of grafted chains Σ, and the (static) friction coefficient f_{mono} between a monomer of the grafted chain and the surrounding matrix. As N increases, additional stress will be required to fracture the interface and eventually a chain scission mechanism will become active. For longer grafted chains at low Σ, the interface will fail when there is sufficient force, f_b, on the backbone of the grafted chains to cause chain scission and fracture will occur when the interfacial stress exceeds $\sigma_{scission} = f_b\Sigma$. As Σ increases, the areal density of entanglements between the grafted brush and the matrix will provide effective enough stress transfer across the interface to cause large scale plastic deformation. In our case, the stress required to craze the thermoplastic, σ_{craze}, is less than the yield stress of the thermoset and we expect a transition from chain scission to crazing at Σ_c. As the stress is increased further,

* To whom correspondence should be addressed.
[†] Current address: Motorola, Inc., MD CH200, 1300 N. Alma School Rd., Chandler, AZ 85224.
[‡] Current address: Institute of Macromolecular Chemistry, Heyrovsky, Sq. 2, 162 06 Prague 6, Czech Republic.
[§] Current address: Xerox Corp., 800 Phillips Rd., Rochester, NY 14580.
[∥] Current address: Motorola, Inc., 5005 E. McDowell Rd., Phoenix, AZ 85008.
[⊥] Current address: Corporate Research and Development, General Electric, P.O. Box 8, Schenectady, NY 12301.
[⊗] Abstract published in *Advance ACS Abstracts,* February 1, 1995.

0024-9297/95/2228-1999$09.00/0

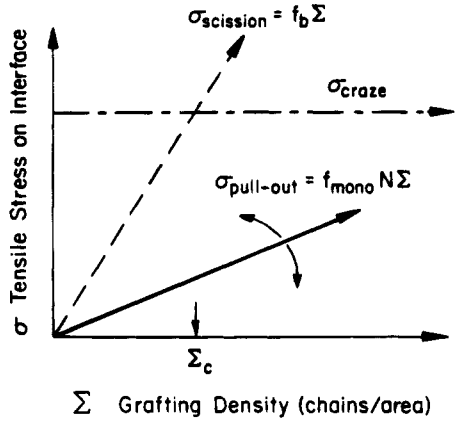

Figure 1. Tensile stress on the interface, σ, plotted versus the grafting density of chains anchored by one end to the interface, Σ. The PS craze widening stress is shown with a dot-dashed line. The stress required to break the backbone bonds of the grafted chains is shown with a dashed line. Pull out of the grafted chains from the PS matrix requires the stress shown with a solid line.

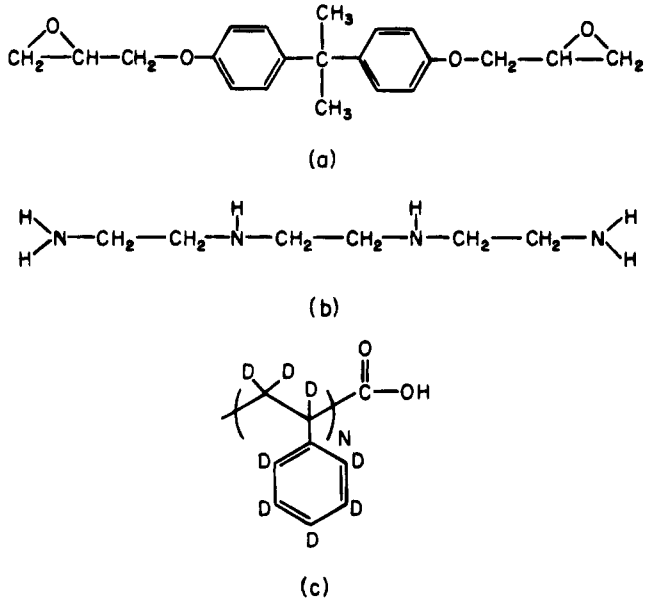

Figure 2. (a) Thermoset resin, diglycidyl ether of Bisphenol A (DGEBA), manufactured by Dow Chemical Co., DER332. (b) Thermoset hardener, triethylenetetramine (TETA), DEH24. (c) Carboxylic acid terminated deuterated polystyrene (dPS-COOH) with degree of polymerization N.

fracture of samples with $\Sigma > \Sigma_c$ will occur by craze failure via pull out of the grafted chains from the craze fibrils or by scission of chains in the fibril structure.

2. Experimental Section

2.1. Materials. The thermoset for this study was constructed from the epoxy resin diglycidyl ether of Bisphenol A (DGEBA) having a molar mass of 350 g/mol. The structure of the resin and that of the curing agent triethylenetetramine (TETA) are shown in Figure 2. The main cure reaction between the resin and hardener is shown in Figure 3a. For the thermoplastic, commercial grade polystyrene (PS) was purchased from Aldrich Chemical Co. with a number average degree of polymerization of 1500 and a polydispersity index of 2.1 as measured by gel permeation chromatography (GPC).

Carboxylic acid terminated deuterated polystyrene (dPS-COOH) was chosen as the adhesion promoter for several reasons. Synthesis via anionic polymerization[12] could be used to prepare a range of dPS molecular weights having narrow molecular weight distributions. In addition, the polystyrenyl

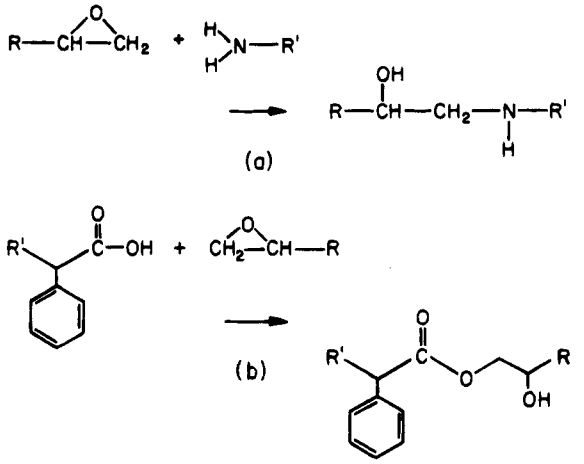

Figure 3. (a) Main cure reaction. (b) Possible grafting reaction.

Table 1. Weight Average Degree of Polymerization N, Weight Average Molar Mass M_w, and Polydispersity Index M_w/M_n of the Carboxylic Acid Terminated Deuterated Polystyrene (dPS-COOH)

N	159	412	535	688	838	1478	1788
M_w	16 580	42 895	55 690	71 500	87 140	153 670	186 000
M_w/M_n	1.03	1.02	1.04	1.07	1.1	1.06	1.2

anion can be reacted with CO_2 to provide a carboxylic acid chain end.[13-16] The −COOH functional group is known to bond with reactive sites in thermoset systems; for example, liquid modifiers such as carboxyl-terminated polybutadiene/acrylonitrile (CTBN)[17] can be incorporated into thermosets. A possible grafting reaction of the carboxylic acid chain end is shown in Figure 3b. Labeling the end-anchored chains with deuterium allows both the grafting density on the interface and the location of chains after fracture to be determined so that the failure mechanism can be monitored. Deuterated styrene was purchased from Aldrich Chemical Co. (98 atom % deuterium), filtered through activated alumina to remove inhibitors, and distilled away from CaH_2 just prior to use. A 100 mL round bottom flask was attached to a vacuum line, evacuated, and then refilled with dry nitrogen. In the flask 5 g of deuterated styrene monomer, 35 mL of dry cyclohexane (passed over activated alumina prior to use), and 15 mL of dry tetrahydrofuran (THF, passed over activated alumina prior to use) were combined, and protic impurities were removed by titration with a *sec*-butyllithium solution (in cyclohexane). Polymerization was initiated with the addition of a *sec*-butyllithium solution and was accompanied by formation of the red color characteristic of polystyrenyllithium and a slight polymerization exotherm. After polymerization for 1 h, stirring was discontinued and the nitrogen atmosphere was replaced with CO_2. Termination of the chain ends was monitored by disappearance of the red anion color, which required between 15 and 60 min. The polymers were then precipitated into methanol containing 5 volume % concentrated hydrochloric acid (to convert CO_2Li end groups to CO_2H) and dried in a vacuum oven to remove residual solvent. Molecular weights were determined by GPC with THF effluent flowing at a rate of 1.0 mL/min through six GPC columns (three mixed porosity, three single pore size), and output was detected using both UV and refractive index detectors. The GPC elution volume/molecular weight response was calibrated using narrow molecular weight polystyrene standards. Molecular weights and polydispersity indices for the dPS-COOH samples are listed in Table 1.

2.2. Interface Preparation. The resin was first heated above 45 °C in a flask to melt any crystalline material. The hardener was added and then stirred under a roughing vacuum to remove bubbles created during mixing. The stoichiometry of the mixture was calculated by assuming each amine hydrogen of the curing agent reacts with one epoxide group of the resin and that no side reactions occur. The epoxy

formulation contained a 50% molar excess of amine hardener or a stoichiometry $S = 1.5$. By varying the epoxy preparation it was possible to manipulate Σ. In general, higher values of Σ were obtained when mixing was stopped close to the gel point. Here we describe the most common interface preparation and will point out important modifications on the procedure where necessary.

To ensure flat epoxy surfaces, the mixture was poured into molds constructed from two pieces of 1/4 in. thick glass sandwiched around a polytetrafluoroethylene (PTFE) spacer. Using cleaning and deposition techniques presented elsewhere,[8] the glass was coated with a self-assembled monolayer as a mold release agent produced from octadecyltrichlorosilane (OTS). The epoxy was then subjected to a B-stage cure in air for 2 h at a temperature between 70 and 120 °C. After the epoxy was removed from the mold, at least a 1000 Å thick film of the end-functionalized polystyrene was deposited on the surface. Most of dPS-COOH films were spun cast from toluene after the solution, typically less than 3 weight % polymer, was allowed to stand for 30 s on the epoxy, a step that initially we thought would ensure more uniform coverage of the epoxy. Some samples were constructed with a solventless transfer technique where the dPS-COOH solution was spun cast onto a glass plate, floated onto the surface of a water bath, and transferred by bringing the epoxy into contact with the floating film from above. To provide the −COOH groups with the mobility to diffuse to the epoxy surface, the bilayers were annealed at 160 °C, well above the glass transition temperature for PS, for up to 20 h. The unanchored chains were removed by washing in tetrahydrofuran in an ultrasonic bath for 20 min with a final squirt bottle rinse with fresh solvent, followed by a drying step of at least 2 h at 80 °C under roughing vacuum.

The interface was then formed against a compression-molded slab of PS at 160 °C for 2 h under contact pressure to allow the tails of the anchored chains to entangle with the PS. The sandwich was cooled, cut with a diamond saw into sticks, and dried at 80 °C under vacuum for at least 2 h before fracture. The final sample geometry consisted of 50 mm long by 7 mm wide strips with epoxy and PS beams of 1.54 mm and 3 mm thickness, respectively.

2.3. Fracture Toughness Measurement. The asymmetric double cantilever beam fracture test was employed to determine the critical energy release rate of an interfacial crack. Since the crazing stress of PS, $\sigma_c = 55$ MPa,[1] is less than the yield stress for similar epoxy,[18] we chose an asymmetric beam geometry.[19,20] This choice maintains crack propagation along the interface, while minimizing craze formation in the PS and preventing fracture of the brittle epoxy. At room temperature in air, a razor blade was inserted at the interface and driven at a constant rate of 3×10^{-6} m/s. From the measured steady state crack length, a, and the expression derived by Creton et al.,[1] which extends Kanninen's[21] description for a beam on an elastic foundation to an asymmetric bimaterial interface, the fracture toughness, G_c, can be computed. Values of Young's modulus used to determine G_c were $E_{ep} = 3500$ MPa for the epoxy[22] and $E_{PS} = 3000$ MPa for PS.[1] The error bars reflect the standard deviation of approximately 16 measurements of G_c made using two different razor blade thicknesses, 0.22 and 0.64 mm. After fracture, forward recoil spectrometry (FRES)[23] was used on the two fracture surfaces to determine the areal density of deuterium atoms. The areal chain (grafting) density, Σ, was computed from the total deuterium areal density of both surfaces.

3. Results and Discussion

3.1. Fracture. The fracture toughness of the bare interface was measured as a baseline against which to compare G_c of our grafted brush modified interfaces. The interface preparation procedure described above was followed, spin casting pure toluene onto the epoxy of the bare interface to mimic the effects of the solvent during the deposition of the end-functionalized dPS. The fracture toughness was consistently 4 ± 0.5 J/m^2 for a variety of epoxy mixing and cure conditions.

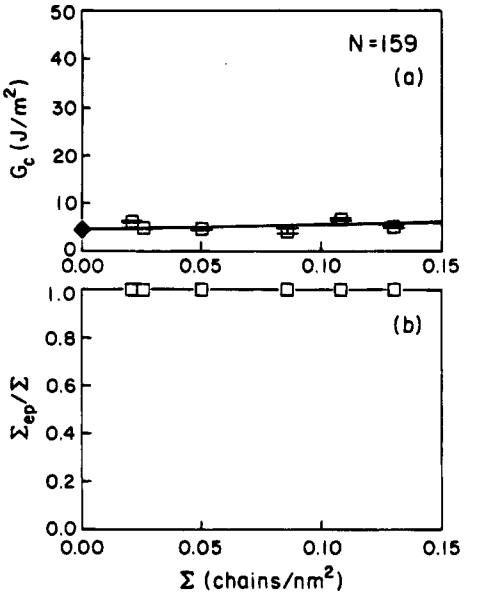

Figure 4. (a) Fracture toughness, G_c, plotted versus the grafting density, Σ, of dPS-COOH chains with $N = 159$ on epoxy prepared with $S = 1.5$. (b) Fraction of deuterium found on epoxy fracture surface Σ_{ep}/Σ plotted versus Σ. Samples prepared via spin casting dPS-COOH onto the epoxy are shown with open squares and via water floatation with solid squares. Lines are provided as a guide.

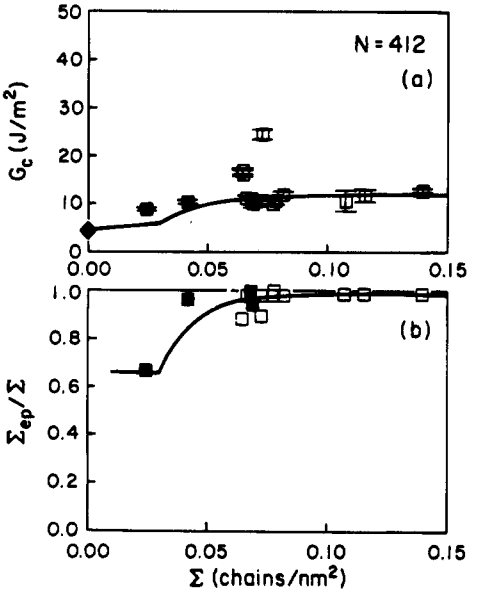

Figure 5. Results for $N = 412$, $S = 1.5$. The symbols are identified in Figure 4.

The results for each chain length are presented in Figures 4–10. The shortest anchored chains used for this investigation had length $N = 159$, just less than the length for entanglement in PS, $N_e = 173$.[24] In Figure 4a almost no enhancement in G_c occurs with increasing grafting density over the bare interface strength, shown with a diamond. In Figure 4b, the fraction of the deuterium found on the epoxy fracture surface, Σ_{ep}/Σ, is plotted versus Σ. In all samples the deuterium is found completely on the epoxy, signifying interface failure via the pull out mechanism. In some samples the frictional force necessary for chain pull out causes a slight increase in G_c over the bare interface value. Optical micrographs of the fracture surfaces revealed no roughness typical of plastic deformation in the interface region. This result agrees with the expectation that chains that are not sufficiently en-

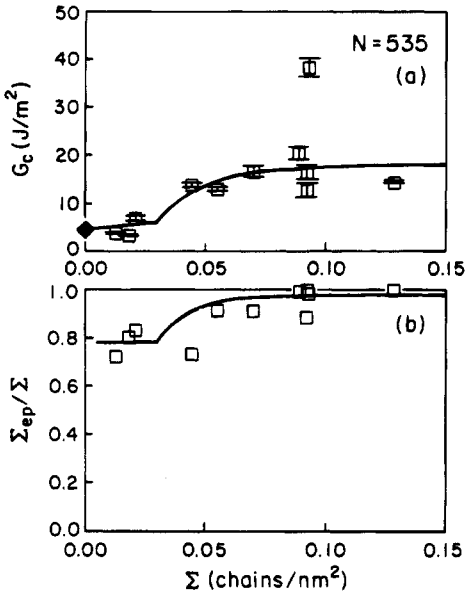

Figure 6. Results for $N = 535$, $S = 1.5$. The symbols are identified in Figure 4.

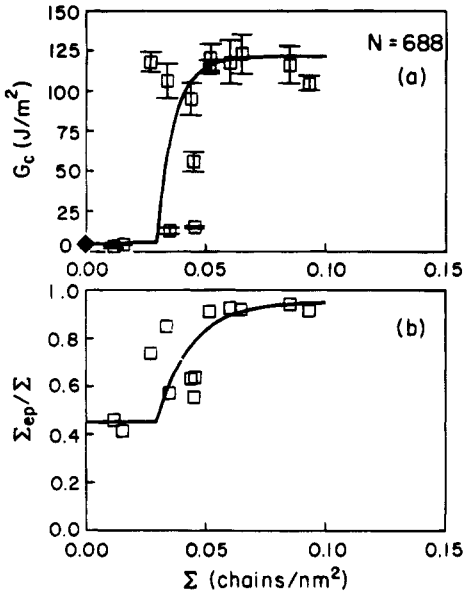

Figure 7. Results for $N = 688$, $S = 1.5$. The symbols are identified in Figure 4.

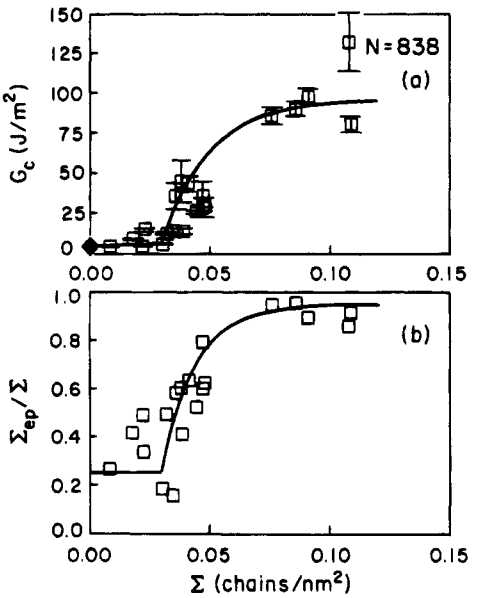

Figure 8. Results for $N = 838$, $S = 1.5$. The symbols are identified in Figure 4.

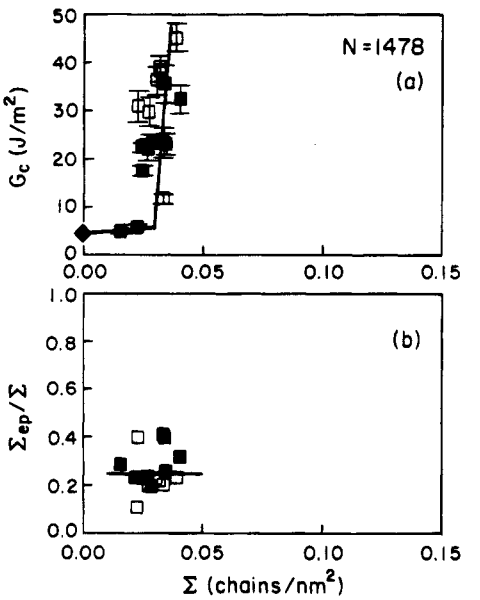

Figure 9. Results for $N = 1478$, $S = 1.5$. The symbols are identified in Figure 4.

tangled provide little stress transfer across the interface, resulting in a weak adhesion and a low G_c value.

At the lowest Σ values for $N = 1478$, chains more than 8 times longer than N_e, G_c increases approximately linearly (Figure 9a). Starting at grafting densities of approximately 0.03 chains/nm^2, there is a sharp increase in G_c leading to an enhancement of the fracture toughness to a value more than 10 times that of the bare interface. This dramatic increase correlates with the onset of large scale energy dissipation through the formation of crazed PS ahead of the crack tip. Optical microscopy revealed roughening of the fracture surfaces, consistent with crazing.[1] Over the entire range of Σ measured, most of the deuterium was found on the PS fracture surface with approximately 20% remaining on the epoxy (Figure 9b). This result is characteristic of scission of the grafted chains close to the epoxy/PS interface. The interface failure of samples prepared via spin casting of the dPS-COOH onto the epoxy in the region of the transition (open symbols of Figure 9) is similar to those samples prepared with water floatation (solid symbols).

Similar behavior is seen in interfaces modified using grafted chains of $N = 688$ (Figure 7) and $N = 838$ (Figure 8). For both dPS-COOH samples we were able to prepare higher Σ samples that allowed further investigation of the interface deformation at fracture. There is a sharp increase in G_c at ≈0.03 chains/nm^2, reaching values of more than 20 times that of the bare interface. A transition in failure mechanism is seen at the same Σ where G_c sharply increases in the plots of Σ_{ep}/Σ. At low Σ the grafted chains break near the interface but the deuterium distribution gradually shifts to larger values of Σ_{ep}/Σ with increasing Σ, leveling off with 90% of the deuterium found on the epoxy fracture surface. This result points to fracture occurring within the craze at the interface between the grafted brush and the PS homopolymer above Σ_c in these samples with intermediate length grafted chains.

To summarize briefly, for three different length grafted brushes a transition is seen from chain scission

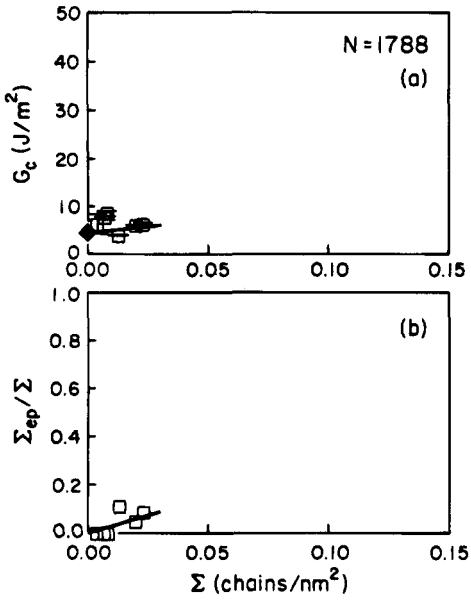

Figure 10. Results for $N = 1788$, $S = 1.5$. The symbols are identified in Figure 4.

to crazing at $\Sigma_c \approx 0.03$ chains/nm^2, demonstrating that Σ_c is independent of N as predicted by the fracture mechanism map. Although the transition to crazing in our system shows some width around Σ_c, it agrees well with Σ_c observed for the interface between PS and poly(2-vinylpyridine) (PVP) modified with PS-*b*-PVP when both blocks are longer than their respective entanglement molecular weights.[1]

The longest grafted chains used had $N = 1788$. For these interface preparations only an extremely limited Σ range was achieved, producing little or no increase in G_c over the bare interface (Figure 10a). Deuterium was found completely on the PS fracture surface in all samples, showing interface failure via chain scission at the epoxy/PS interface. These results and the deuterium distribution seen in the $N = 1478$ samples are similar to observations by Creton et al.[6] of block copolymer modified interfaces. For well-entangled chains interface failure occurs not at the brush tip–craze interface but near the grafted chain end or near the joint of the block copolymer. The limited Σ achieved both in the $N = 1788$ case and for $N = 1478$ is in part the consequence of an entropic barrier to grafting and will be discussed in detail below.

For intermediate length grafted chains, $N = 412$ and 535, 2.3 and 3 times the entanglement length, respectively, there is sufficient entanglement to produce the gradual increase in G_c with Σ seen in Figures 5 and 6. For both cases G_c reaches a constant value of approximately 11 J/m^2 for $N = 412$ and 16 J/m^2 for $N = 535$. From the deuterium distribution on the fracture surfaces of both interface types we observe some samples that fail by chain pull out, $\Sigma_{ep}/\Sigma = 1$, as well as some that fail by chain scission $\Sigma_{ep}/\Sigma < 1$. Smooth fracture surfaces were observed with optical microscopy for the $N = 412$ samples with $G_c \approx 11$ J/m^2 and rough fracture surfaces for the samples with G_c greater than the plateau value. The $N = 535$ samples consistently showed roughening of the fracture surfaces for $\Sigma > 0.05$ chains/nm^2. This texture is typical of the crazed PS formed ahead of the crack tip. The small enhancement in G_c over the bare interface for the $N = 535$ brushes compared with those with $N > 688$ and the rough fracture surfaces agrees with previous observations of craze instability in low molecular weight bulk PS.[25] Thus, for the $N = 412$ and 535 samples the chains are sufficiently well entangled to allow a craze to form in the PS, however the craze that forms is weakly coupled to the interface and breakdown occurs in the craze fibrils either by chain pull out or chain scission.

In the $N = 412$ and $N = 535$ data, several samples had G_c values that are distinctly different from the average behavior. Furthermore, the maximum G_c value observed for these chain lengths are unexpectedly lower than the fracture toughness for PS/PVP interfaces modified with block copolymers where both block lengths are comparable to the end-anchored chains using N_e as a reference. For example, the bare PS/PVP interface has a fracture toughness of about 1 J/m^2 which is increased to 22 J/m^2 with the addition of 510-*b*-540 PS-*b*-PVP at $\Sigma = 0.1$ chains/nm^2. Similarly, for 800-*b*-870 at the same Σ, $G_c = 80$ J/m^2.[4] In addition, if we compare the failure mechanism of the $N = 412$ and $N = 535$ dPS-COOH modified epoxy–PS interfaces with the PS–PVP interface we find another mismatch. 510-*b*-540 and 800-*b*-870 both show a clear transition in the deuterium distribution from chain scission at the interface to crazing with failure at the block copolymer brush interface with the homopolymer. For the samples measured we do not see comparable behavior until $N = 688$. From the fracture mechanism map and previous block copolymer experiments we can estimate the N where we would first expect to see evidence of Σ_c.

From experiments by Washiyama et al.,[26] with a PS-*b*-PVP block copolymer that shows a transition from block pull out from the PVP to crazing of the PS, they were able to quantify the static frictional force required per monomer for pull out, $f_{mono}^{PVP} = 6.3 \times 10^{-12}$ N/mer. Since PS and PVP are both glassy polymers, where the yield stress of PS, σ_y^{PS} is similar or slightly less than σ_y^{PVP} it is reasonable to assume that $f_{mono}^{PS} \leq f_{mono}^{PVP}$. From Σ_c and the fracture mechanism map, Creton et al.[1] estimate the force to break a C–C bond of the PS backbone to be $f_b \approx 2 \times 10^{-9}$ N/bond. From these values, at low Σ we should expect to see a transition from pull out of the grafted chains to scission when $\sigma_{pullout} = \sigma_{scission}$ or when $N^* = 350$. However, investigations of chain pull out fracture revealed that when $N_e < N < N^*$ there is an extra friction force because of entanglements in addition to the static friction force used to predict N^*.[27] Therefore, the signature of pure pull out, $\Sigma_e/\Sigma = 1$, should occur only for samples with $N < N_e$. Indeed, this is observed for $N = 159$ but, using the values of f_{mono} and the PS crazing stress σ_c, we also expect to see a transition from pull out to crazing at $\Sigma^* = 0.055$ chains/nm^2. Our experiments show no hint of such a transition like that seen with 580-*b*-220 PS-*b*-PVP at a PS–PVP interface, when both G_c and Σ_{ep}/Σ would show a discontinuity at Σ^* with the onset of large scale energy dissipation through formation of crazes.[26] Additionally, interface failure by scission is not uniformly observed for all samples with $N = 412$ and $N = 535$, both having $N > N^*$; more definitive evidence of chain scission is seen when $N = 688$. These inconsistencies may be explained if the dPS-COOH penetrates the epoxy surface, resulting in effectively shorter tails available for stress transfer through entanglement with the PS homopolymer chains. Therefore, we next investigated the detailed structure of the epoxy–PS interface using a combination of direct space profiling (FRES) with high-resolution neutron reflectometry.

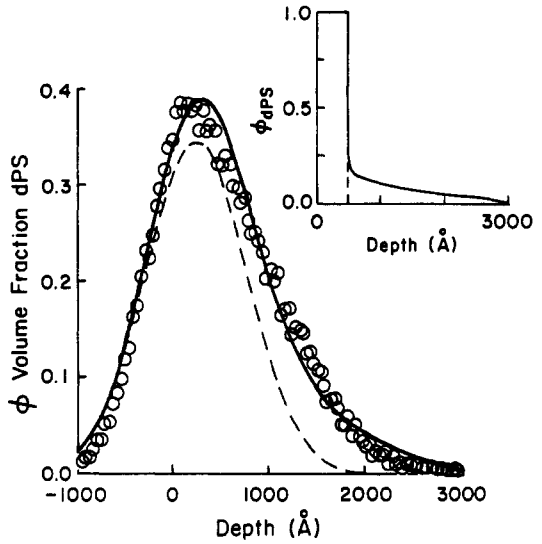

Figure 11. Forward recoil spectrum of an interface between epoxy of $S = 1.5$ and pure dPS, $N = 1800$. The dashed line assumes a uniform dPS film of thickness 485 Å. The solid line assumes a uniform dPS film on the epoxy with a decay of the dPS volume fraction, ϕ, to a depth of more than 2500 Å into the epoxy. Both profiles are smeared by a Gaussian with a width of 480 Å.

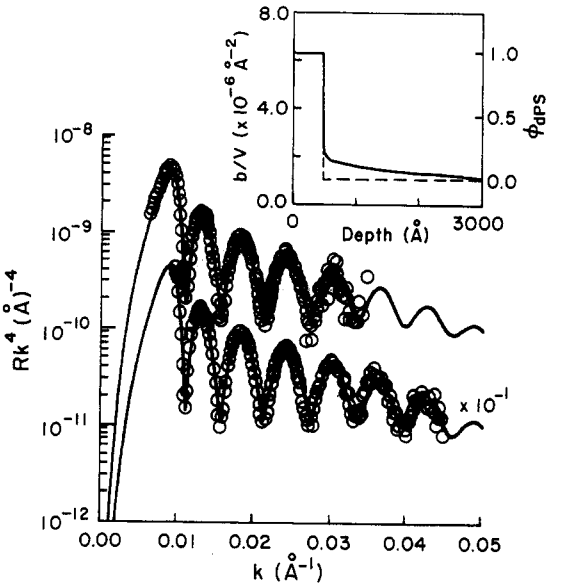

Figure 12. Neutron reflection spectra from an interface between epoxy with $S = 1.5$ and pure dPS, $N = 1800$, plotted as Rk^4 versus k where the R is the neutron reflectivity and k is the perpendicular component of the neutron wave vector. Data taken at two incident angles 0.88 and 1.29° are offset for clarity. The solid line is a fit to the data based on the solid line scattering length density b/V or volume fraction ϕ profile shown in the inset.

3.2. Interface Width. For detailed profiling of the interface with neutron reflectometry (NR), a technique reviewed in detail elsewhere,[28] the epoxy mold was altered slightly to produce a sample with minimal curvature, as this curvature would cause a decrease in the resolution of the neutron reflection technique. A 2 in. diameter by $^3/_{16}$ in. thick silicon single crystal was used to provide a rigid support for the interface. This wafer was recessed in a hole slightly below the surface of a PTFE block. The epoxy mixture was poured on top of the silicon and another $^1/_4$ in. thick silicon wafer, coated with OTS, was pressed onto the epoxy mixture and then subjected to 85 °C for 2 h. This procedure created a film ≈10 μm thick. To produce a sharp contrast in deuterium content at the interface, and thus neutron scattering length density b/V, we replaced both the end-functionalized polymer and the polystyrene homopolymer with commercially available monodisperse dPS, $N = 1800$, purchased from Polymer Laboratories. The dPS was spun cast from toluene onto the epoxy after the solution was allowed to stand on the surface for 30 s, a typical interface preparation that we felt might result in the most severe penetration of the dPS into the epoxy. This sample was allowed to dry in air for 5 h before it was annealed at 160 °C for 1 h. It was then washed for 40 min in THF, dried, and subsequently coated again with ≈500 Å for $N = 1800$ dPS. It was then annealed for 2.5 h at 160 °C to simulate the interface welding step done for the fracture specimens.

Figure 11 shows the deuterium signal measured as a function of depth with FRES. The dashed line assumes a uniform 485 Å thick dPS film on top of the epoxy smeared by a Gaussian. From a comparison with the data one sees that there is substantial penetration of dPS into the epoxy to a depth of ≈2500 Å. Since the resolution of FRES is poor, we used NR to probe the interface structure in more detail. In Figure 12 the reflection spectrum taken at two incident angles is plotted as Rk^4 versus k where R is the neutron reflectivity and k is the perpendicular component of the neutron wave vector. The solid line through the data is calculated on the basis of the b/V profile shown in the inset with a solid line. The oscillations in the data are the result of interference between waves reflected from the air surface and from the dPS–epoxy interface. The period is inversely related to the dPS film thickness found to be 485 Å in this sample. The decay of the amplitude of the oscillations with increasing k is sensitive to the contrast between the scattering length density of the pure dPS layer, $(b/V)|_{dPS} = 6.28 \times 10^{-6}$ Å^{-2}, and that of pure epoxy, $(b/V)|_{ep} = 1.04 \times 10^{-6}$ Å^{-2}, the value calculated from the density of epoxy. Simulations of the reflectivity assuming no penetration of dPS into the epoxy (dashed line profile of the inset) do not fit the decay of the oscillation amplitude. A volume fraction of dPS in the epoxy at the interface of $\phi = 0.267$ with an interface roughness of 30 Å dramatically improves the fit and is presented in Figure 12. Profiles comparable to that measured by FRES, a gradual decay from $\phi = 0.267$ at the interface to $\phi = 0$ over ≈2500 Å into the epoxy, produce reflectivity spectra indistinguishable from profiles with a uniform distribution of dPS at $\phi = 0.267$ throughout the epoxy. This ambiguity is a consequence of NR's sensitivity to sharp gradients in b/V. The results from both FRES and NR validate our suspicion that the interface is diffuse and the brush molecules anchor beneath the epoxy surface.

3.3. Grafting. For interfaces with the longest end-anchored molecules, $N = 1788$, we were not able to produce samples with $\Sigma > \Sigma_c$ where energy dissipation occurs through the formation of crazed PS. When we plot the maximum grafting density achieved for the fracture studies, Σ^{max}, for each length of grafted chain in Figure 13, a clear trend emerges. There is a nearly linear decrease in the Σ^{max} with the increasing degree of polymerization. The same trend is also observed in experiments where parallel samples, undergoing identical grafting conditions, with dPS-COOH of varying N are grafted to epoxy cut from the same slab. We briefly explore the thermodynamics of grafting end-functionalized polymers to an interface and the dependence of the ultimate grafting density on the chain length.

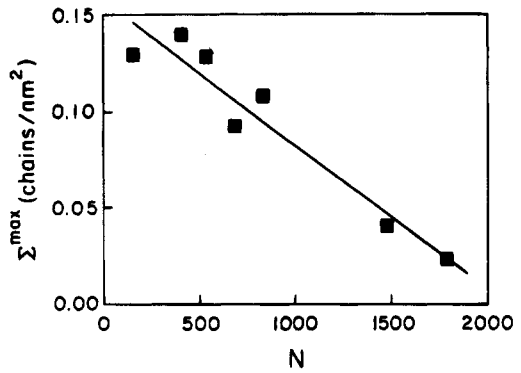

Figure 13. Maximum value of the grafting density, Σ^{max}, obtained in fracture experiments plotted versus the degree of polymerization, N, of dPS-COOH. The line is a linear fit to the data.

In our interface preparation the grafted brush is constructed by drawing chains from a thick film reservoir of dPS-COOH. If we treat the grafted brush polymers as a separate phase from the unanchored chains, the chemical potential for a grafted chain, μ, can be written using notation of Shull[29]

$$\frac{\mu}{k_B T} = \frac{\Delta f_{rxn}}{k_B T} - 1.1 \ln\left(\frac{\delta}{R_g}\right) + \frac{\mu_{st}\left(\frac{z^*}{R_g}\right)}{k_B T} \qquad (1)$$

The first term accounts for the free energy of the grafting reaction. The entropy lost with confinement of the chain end to a region of interface width δ is given by the logarithm term, where R_g is the radius of gyration of the dPS chain. The entropy penalty of stretching the grafted molecule to accommodate other chains in the brush is $\mu_{st}/k_B t$, a function of the normalized coverage of the epoxy surface, z^*/R_g, where $z^* = N\Sigma/\varrho_0$ and ϱ_0 is the segment density. The chemical potential for a chain just before anchoring, with its end located a distance from the wall equal to the statistical segment length, a, is given by

$$\frac{\mu^*}{k_B T} = -1.1 \ln\left(\frac{a}{R_g}\right) + \frac{\mu_{st}\left(\frac{z^*}{R_g}\right)}{k_B T} \qquad (2)$$

Thus, $\mu^*/k_B T$ is the height of the potential barrier that a chain end must overcome to reap the energetic gain of the grafting reaction, $\Delta f_{rxn}/k_B T$. The barrier height can be calculated using results of Shull[29] who carried out numerical calculations for end-anchored chains in a melt using self-consistent mean field theory. Shull's tabulated values for $\mu_{st}/k_B T$ for grafted chains much shorter than the matrix polymer are used in Figure 14 to calculate the lines of constant barrier height in the graph of normalized coverage versus chain length. The symbols come from Σ^{max} of the G_c experiments normalized with the appropriate R_g. Except for $N = 159$, the general trend of the data agrees with the thermodynamic prediction of a monotonic decrease of the equilibrium coverage with increasing chain length. In other grafting experiments with $N = 159$ we have observed values of z^*/R_g as high as 1.88, which is more in line with the behavior of the intermediate length grafted chains. Thus, for increasingly long molecules, a potential barrier opposing the addition of new chains limits the ultimate grafting density. This limited tethering

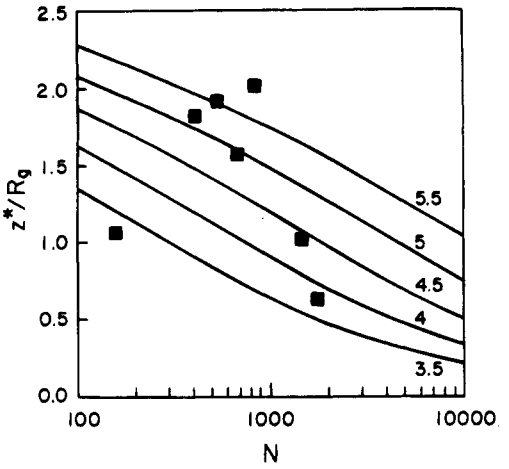

Figure 14. Normalized interfacial coverage, z^*/R_g, plotted against the logarithm of the degree of polymerization, N. Noted next to each line is $\mu^*/k_B T$, the height of the chemical potential barrier used to calculate each curve. The symbols are calculated from the maximum value of the grafting density achieved in our preparations of the fracture interfaces.

of chains to a wall has been more cleanly observed in studies of adsorption of block copolymers from solution.[30]

In our system, if only one chemical reaction is active between the dPS-COOH chains and the epoxy, Δf_{rxn} should be the same in all samples and at equilibrium the height of the barrier μ^* should be constant across all samples. This is not the case, especially for $N = 1478$ and 1788 in Figure 14. As alluded to in the description of the interface construction, Σ does depend on the preparation of the epoxy: mixing temperature, mixing time, B-stage curing conditions, and presumably stoichiometry. In the $N = 1478$ experiments many unsuccessful attempts were made to produce samples with $\Sigma \gg \Sigma_c$. This evidence led to an exploration of the grafting mechanism via a study of the kinetics of brush formation.

As chains graft to the epoxy, the kinetics should reflect the time necessary for a new chain to penetrate the existing brush.[31] Assuming the grafting reaction is irreversible (i.e. Δf_{rxn} is strongly negative), we ignore the flux of chain ends desorbing from the wall. The flux of chain ends arriving at the wall, J_{in}, is then identical to the grafting rate, $d\Sigma/dt$, and depends on the diffusion coefficient, D, of dPS in PS and the change in n, the –COOH concentration, over distance x from the wall

$$J_{in} = \frac{d\Sigma}{dt} = -D\frac{dn}{dx} \qquad (3)$$

The density of ends in the bulk, far away from the interface, is $n_\infty = \varrho_0/N$. In the grafted brush there will be a depletion in the density of reactive end groups that is related to the chemical potential. At a distance a from the wall, n depends on the chemical potential barrier height as

$$n(a) = n^* = n_\infty \exp\left(-\frac{\mu^*}{k_B T}\right) \qquad (4)$$

Over the interface width a where grafting occurs, $-dn/dx \approx n^*/a$ since the ends have reacted right at the epoxy surface ($n(0) = 0$). Combining the above expressions and rewriting the result in terms of the normalized interfacial coverage, $\xi = z^*/R_g$, we can integrate to arrive

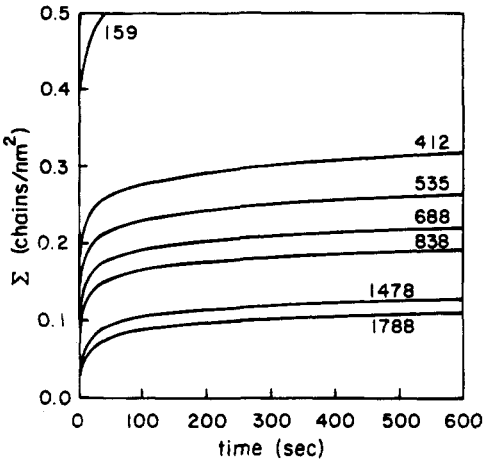

Figure 15. Grafting density predicted as a function of time for different chain lengths, N, noted next to each curve.

at the following time dependence of grafting

$$\int_0^{\xi} d\xi \exp\left(\frac{\mu^*(\xi)}{k_B T}\right) = \frac{t}{\tau_0} \quad (5)$$

The parameters of the characteristic time $\tau_0 = R_g a/D$ have been measured for PS at 160 °C.[32,33] The kinetics based on the above prediction are plotted in Figure 15. The rate of grafting is large over the first 50 s but then slows down to produce a gradual increase in Σ with continued annealing. Shorter chains reach higher grafting densities faster than longer chains. This trend with chain length agrees with both grafting experiments using dPS-COOH with several values of N grafted to pieces of the same epoxy for a fixed annealing time and with the monotonic decrease we see in the fracture experiments of Σ^{max} with N (Figure 13). However, the predicted grafting density is considerably larger than that of any samples we made.

To test the general shape of these curves and the time scale over which grafting occurs, epoxy was prepared by following steps that have been observed to give the largest Σ. Two batches of epoxy were mixed, bringing them close to the gel point, at 52 °C for 17 min for S = 1.5 and 49 °C for 17 min for S = 0.75. They were allowed to sit at room temperature overnight and then cured at 120 °C for 2 h. A layer of dPS-COOH of N = 838 was deposited by spin casting onto a large plate of each epoxy. The plate was then broken by cleaving into multiple pieces, each annealed at 160 °C for different amounts of time and washed for 20 min in THF to remove unreacted chains. The open symbols of Figure 16 show the grafting density measured by FRES plotted against the time allowed for the ends to anchor to the S = 1.5 epoxy. A sharp increase in Σ occurs in the first 180 min, and then the rate of anchoring slows. The scatter and the data point at 2800 min, which shows a lower Σ, may result from inhomogeneities in the epoxy surface. The same curve shape has also been measured for N = 688 end-functionalized polymer up to 800 min where most of the grafting occurred in the first 60 min. In general, the shape is remarkably similar to that predicted from our simple model of the chain end diffusion through the grafted brush at short annealing times, although the time scales differ by nearly 1 order of magnitude and the experimental Σ's are much lower than predicted. The difference in time scale suggests that end-anchoring is not limited by the diffusion time for chain ends to reach a grafting site in or on the epoxy.

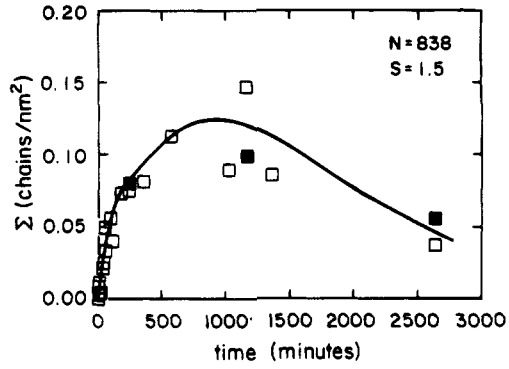

Figure 16. Grafting density obtained versus annealing time at 160 °C of a pure layer of N = 838 dPS-COOH on amine rich, S = 1.5, epoxy. The open symbols are the Σ value with one deposition of dPS-COOH and annealing. The solid symbols are samples annealed for the time indicated on the x-axis with the additional surface treatment of a second spun cast layer of dPS-COOH annealed at 160 °C for an additional 920 min and then washed. The line is provided as a guide.

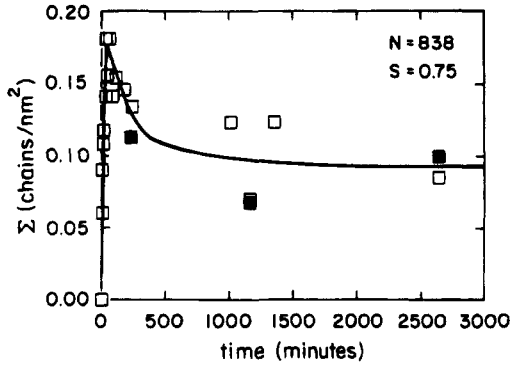

Figure 17. Grafting density obtained versus annealing time at 160 °C of a pure layer of N = 838 dPS-COOH on epoxide rich, S = 0.75, epoxy. The open symbols are the Σ value with one deposition of dPS-COOH and annealing. The solid symbols are samples annealed for the time indicated on the x-axis with the additional surface treatment of a second spun cast layer of dPS-COOH annealed at 160 °C for an additional 920 min and then washed. The line is provided as a guide.

When the epoxy stoichiometry is changed to have an excess of resin, S = 0.75, the grafting kinetics shows a very different behavior (Figure 17). There is a faster rate of grafting in the initial 60 min of annealing than that for the S = 1.5 stoichiometry, but Σ reaches a peak value of 0.18 chains/nm² before it falls off to 0.10 chains/nm². The initial rate of grafting is comparable to the prediction from diffusion-controlled grafting up to the time where Σ begins to decrease. This time dependence was also observed for N = 688, with the peak occurring at nearly the same time. The decrease in Σ at long annealing times implies that another chemical reaction causes some ungrafting of the end-anchored chains and prevents subsequent reanchoring. That Σ does not increase with time in either stoichiometry as predicted also suggests that maybe the availability of grafting sites in or on the epoxy has been depleted by the 160 °C treatment, which effectively completes the cure, or the reactivity of the −COOH ends has degraded.

The interaction of the −COOH acid with the strong basic amine groups, primary and secondary, of the epoxy network is known to lead to deprotonation and creation of a carboxylate anion. The negative charge is spread over the three atoms of the carboxylate making attack of the sheltered carbonyl carbon by the nitrogen to form an amide extremely unlikely. Upon annealing at 160 °C, two processes are likely to compete. The carboxylate

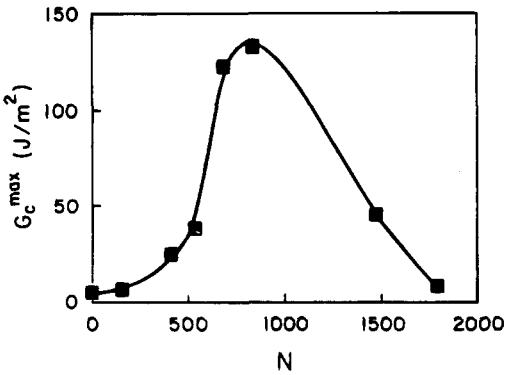

Figure 18. Maximum fracture toughness, G^{max}_c observed in fracture experiments versus the degree of polymerization, N, of the dPS-COOH grafted chains. The line is a spline fit to the data.

anion may attack residual epoxides, although in the amine rich ($S = 1.5$) epoxy samples this may not occur as readily since the amine is a stronger nucleophile than the carboxylate anion. The other possible process is decarboxylation of the polystyrene, probably in the presence of the ammonium ion leading to loss of CO_2 and the formation of a polystyrenyl anion stabilized by the benzene ring. If the ends are deactivated for this or another reason, replenishing the reservoir with fresh dPS-COOH may lead to higher Σ. To test this hypothesis, three epoxy chips from each stoichiometry were selected for a second surface treatment. A layer of end-functionalized polymer was spun cast on top of the existing grafted layer, annealed for 920 min at 160 °C, and washed, and the Σ data were measured. These samples are shown as the solid squares in Figures 16 and 17 at the annealing time of the first dPS-COOH deposition. Essentially no increase in Σ is observed. This result implies that after the formation of the brush the epoxy reactivity becomes important to continued buildup of the brush. Changes in the mold surface from OTS to other surfaces (Teflon, Mylar, air, dPS-COOH) or grinding of the epoxy to expose fresh material yielded no increase in Σ and, in many cases, led to a decrease.

The limitation on the grafting density for long chains has the net effect of reducing the maximum obtainable fracture toughness for the longest grafted chain as compared to intermediate chain lengths. In Figure 18, G_c^{max}, the maximum fracture toughness observed, is plotted for each N. There is a peak near $N = 838$ which results from the combination of the decrease in achievable Σ with the increase in N and the variation of the interface failure mechanism with N. In samples with short grafted chains, $N = 159$, large Σs are possible but the interface failure mechanism is chain pullout and the interfaces are weak. At the largest Σ values in samples with $N > N_e$, as N increases, a craze forms ahead of the crack tip. At intermediate chain lengths ($412 \leq N \leq 838$) craze failure occurs partly by chain disentanglement of the grafted chains from the craze. The signature for this failure mechanism is that nearly all of the dPS-COOH is found on the epoxy fracture surface. When N is raised above 838, a transition from craze breakdown by disentanglement to craze failure by chain scission occurs, as signaled by the finding that the dPS-COOH is mostly on the PS fracture surface. In the $N = 1478$ and $N = 1788$ samples, the anchored chains are well entangled but the maximum fracture toughness observed is lower than in the $N = 838$ samples due to the limited Σ achieved, a consequence of a combination of an entropic barrier to grafting and the chemical anchoring mechanisms active in this material system. A similar tradeoff is observed when well-entangled diblock copolymers modify the interface between immiscible thermoplastics.[9] The number of diblock copolymer chains required to form a complete lamellae decreases as the length of the diblock copolymer increases. This space-filling condition therefore limits the number of diblock copolymer chains that cross the interface, decreasing the maximum obtainable toughness as the copolymer length increases. When engineering the toughness of practical interfaces, it will be critical to take such effects into account.

4. Conclusions

A systematic study of the adhesion between a thermoset (epoxy) and a thermoplastic (polystyrene) as the length of end-anchored chains was increased revealed the following results using an asymmetric double cantilever beam fracture test. Carboxylic acid termination is enough to anchor chains to an epoxy surface while the dPS entangles in the PS, increasing the energy per unit area required to fracture the interface by as much as 25 times. The fracture toughness G_c and mechanism of interface failure, determined with FRES, depend on the grafting density Σ and chain length N. For chains with $N < N_e$, no enhancement in G_c over the bare interface is observed and all the deuterium was found on the epoxy fracture surface consistent with interface fracture via chain pullout. The transition from chain scission near the interface to craze failure via scission in the craze fibrils near the grafted brush–craze interface occurred around $\Sigma_c = 0.03$ chains/nm^2 for three different chain lengths. This result is consistent with the prediction from the fracture mechanism map[2] that Σ_c is independent of N and with observations of Σ_c in block copolymer modified polymer interfaces.[1] Some penetration of the dPS-COOH chains into the epoxy is seen with both FRES and NR, effectively shortening the brush molecules available for entanglement and thus stress transfer. As N increases the maximum observed value of Σ decreases approximately linearly. Consequently, the optimum grafted chain length to produce the largest enhancement in G_c was observed for intermediate length grafted chains $N = 838$. These results can be attributed to a combination of an entropic barrier to grafting opposing the addition of new chains to an existing brush and limitations of the particular interface chemistry being exploited in this study.

Acknowledgment. The authors acknowledge support provided by Dow Chemical Co. through the Cornell Polymer Outreach Program and the NSF-DMR MRL Program. L.J.N. was supported by a Department of Education Polymer Fellowship 1991–93. A.H. received funds from the General Electric Foundation Faculty for the Future grant. We would like to thank M. Calistri-Yeh for instructing us in the preparation of OTS coatings of our mold surfaces. Discussions with C.-A. Dai, J. Washiyama, F. Xiao, J. Smith, Y. Sha, C.-Y. Hui, and A. Shank are appreciated. The reflectivity measurements were done at IPNS at Argonne National Laboratory that is funded by the U.S. Department of Energy under contract W-31-109-ENG-38. We benefited from the use of the facilities of the Materials Science Center and the National Nanofabrication Facility at Cornell University that are supported by the NSF.

References and Notes

(1) Creton, C. F.; Kramer, E. J.; Hui, C.-Y.; Brown, H. R. *Macromolecules* **1992**, *25*, 3075.

(2) Xu, D. B.; Hui, C.-Y.; Kramer, E. J.; Creton, C. *Mech. Mater.* **1991**, *11*, 257.
(3) Brown, H. R. *Macromolecules* **1989**, *22*, 2859.
(4) Washiyama, J.; Creton, C.; Kramer, E. J.; Xiao, F.; Hui, C. Y. *Macromolecules* **1993**, *26*, 6011.
(5) Brown, H. R.; Char, K.; Deline, V. R.; Green, P. F. *Macromolecules* **1993**, *26*, 4155.
(6) Creton, C.; Brown, H. R.; Deline, V. R. *Macromolecules* **1994**, *27*, 1774.
(7) Smith, J. W.; Kramer, E. J.; Xiao, F.; Hui, C.-Y.; Reichert, W.; Brown, H. R. *J. Mater. Sci.* **1993**, *28*, 4234.
(8) Calistri-Yeh, M. Ph.D. Thesis, Cornell University, Ithaca, NY, 1995.
(9) Char, K.; Brown, H. R.; Deline, V. R. *Macromolecules* **1993**, *26*, 4164.
(10) Dai, C.-A.; Dair, B. J.; Dai, K. H.; Ober, C. K.; Kramer, E. J.; Hui, C.-Y.; Jelinski, L. W. *Phys. Rev. Lett.* **1994**, *73*, 2472.
(11) Lee, Y.; Char, K. *Macromolecules* **1994**, *27*, 2603.
(12) Morton, M. *Anionic Polymerization, Principles and Practice*; Academic Press: New York, 1983.
(13) Zelinski, R. P.; Strobel, C. W. U.S. Patent **1963**, 3 018 994.
(14) Quirk, R. P.; Chen, W.-C. *Makromol. Chem.* **1982**, *183*, 2071.
(15) Young, R. N.; Quirk, R. P.; Fetters, L. J. *Adv. Polym. Sci.* **1984**, *56*, 1.
(16) Quirk, R. P.; Yin, J.; Fetters, L. J. *Macromolecules* **1989**, *22*, 85.
(17) Drake, R. S.; Egan, D. R.; Murphy, W. T. In *Elastomer-Modified Epoxy Resins*. Bauer, R. S., Ed.; *Epoxy Resin Chemistry II*; American Chemical Society: Washington, DC, 1983.
(18) Glad, M. D. Ph.D. Thesis, Cornell University, Ithaca, NY, 1986.
(19) Brown, H. R. *J. Mater. Sci.* **1990**, *25*, 2791.
(20) Xiao, F.; Hui, C.-Y.; Kramer, E. J. *J. Mater. Sci.* **1993**, *28*, 5620.
(21) Kanninen, M. F. *Int. J. Fract.* **1973**, *9*, 83.
(22) This value is close to literature values of E_{ep} for DGEBA. E_{ep} will depend on the stoichiometry and the degree of network formation (or extent of cure).
(23) Mills, P. J.; Green, P. F.; Palmstrom, C. J.; Mayer, J. W.; Kramer, E. J. *J. Appl. Phys. Lett.* **1984**, *45*, 957.
(24) Onogi, S.; Masuda, T.; Kitagawa, K. *Macromolecules* **1970**, *3*, 109.
(25) Yang, A. C.-M.; Kramer, E. J.; Kuo, C. C.; Phoenix, S. L. *Macromolecules* **1986**, *19*, 2010.
(26) Washiyama, J.; Kramer, E. J.; Hui, C. Y. *Macromolecules* **1993**, *26*, 2928.
(27) Washiyama, J.; Kramer, E. J.; Creton, C.; Hui, C. Y. *Macromolecules* **1994**, *27*, 2019.
(28) Russell, T. P. *Mater. Sci. Rep.* **1990**, *5*, 179.
(29) Shull, K. R. *J. Chem. Phys.* **1991**. *94*, 5723.
(30) Parsonage, E.; Tirrell, M.; Watanabe, H.; Nuzzo, R. G. *Macromolecules* **1991**, *24*, 1987.
(31) Ligoure, C.; Leibler, L. *J. Phys. II* **1990**, *51*, 1313.
(32) Green, P. F.; Palmstrom, C. J.; Mayer, J. W.; Kramer, E. J. *Macromolecules* **1985**, *18*, 501.
(33) Tangari, C.; King, J. S.; Summerfield, G. C. *Macromolecules* **1982**, *23*, 132.

MA941268B